Biochimica et Biophysica Acta 1788 (2009) 1474–1481

Contents lists available at ScienceDirect

Biochimica et Biophysica Acta

journal homepage: www.elsevier.com/locate/bbamem

Interaction of the MARCKS peptide with PIP_2 in phospholipid monolayers

Undine Dietrich [a,*], Peter Krüger [b], Thomas Gutberlet [c], Josef A. Käs [a]

[a] Division of Soft Matter Physics, Faculty for Physics and Earth Sciences, University of Leipzig, Linnéstr. 5, D-04103 Leipzig, Germany
[b] Fraunhofer Institute for Non-Destructive Testing, Dresden Branch, Germany
[c] Forschungszentrum Jülich GmbH, Jülich Centre for Neutron Science, Garching, Germany

ARTICLE INFO

Article history:
Received 30 January 2009
Received in revised form 15 March 2009
Accepted 1 April 2009
Available online 9 April 2009

Keywords:
Peptide/monolayer interaction
Lateral organization
Structural parameter

ABSTRACT

In this present work we have studied the effect of MARCKS (151–175) peptide on a mixed DPPC/PIP_2 monolayer. By means of film balance, fluorescence microscopy, x-ray reflection/diffraction and neutron reflection measurements we detected changes in the lateral organization of the monolayer and changes in the perpendicular orientation of the PIP_2 molecules depending on the presence of MARCKS (151–175) peptide in the subphase. In the mixed monolayer, the PIP_2 molecules are distributed uniformly in the disordered phase of the monolayer, whereas the PI(4,5) groups elongate up to 10 Å below the phosphodiester groups. This elongation forms the precondition for the electrostatic interaction of the MARCKS peptide with the PIP_2 molecules. Due to the enrichment of PIP_2 in the disordered phase, the interaction with the peptide occurs primarily in this phase, causing the PI(4,5) groups to tilt toward the monolayer interface.

1. Introduction

MARCKS proteins are a family of membrane associated proteins, which are involved in a number of signal transduction processes that regulate cell motility, secretion, membrane associated transport as well as the regulation of the cell cycle. All of these processes are related to the reorganization of the actin cytoskeleton [1,2]. Relevant for the regulative function of the MARCKS protein is its so-called effector domain—a sequence of 25 amino acids [3,4]. This effector domain binds reversibly to the plasma membrane and modulates the actin filament assembly [5,6].

Experimental studies have shown strong electrostatic binding of the MARCKS effector domain to membranes containing acidic lipids such as the second messenger phosphatidylinositol 4,5-biphosphate, PIP_2 [7,8]. For this strong electrostatic interaction, the 13 basic amino acid residues of the effector domain are responsible. Additional to this electrostatic interaction, 5 aromatic Phenylalanine (Phe) residues penetrate into the acyl chain layer of the lipid membrane [9–11]. The electrostatic binding of the MARCKS effector domain with the membrane can be inhibited by binding to Calcium/Calmodulin (Ca^{2+}/CaM) or due to phosphorylation by protein kinase C (PKC) [9,11,12]. These reversible translocations—the so-called myristoyl-electrostatic switch [13,14]—permit the regulative function of the MARCKS protein [15,16].

With a variety of techniques, it was found that a peptide sequence containing the 25 amino acid residues analogous to the MARCKS effector domain, the MARCKS (151–175), mimics that electrostatic interaction [3,7–9,17,18] entirely. Hence, this peptide is a well-suited model for studying the interaction of MARCKS with membranes. The structural arrangement of the MARCKS protein and the MARCKS (151–175) peptide in the membrane and the consequential alteration of membrane structure by MARCKS have been studied in recent works [19–25]. However, the applied methods require chemical modifications of the protein/peptide or of the PIP_2 such as dye-labeling [24,25], spin-labeling [20,22,24], or the replacement of amino acid groups [21]. To circumvent the potentially perturbing effects of these modifications, x-ray reflectivity experiments have been used to investigate the interaction of proteins with lipid monolayers at the air–water interface, mimicking the inner leaflet of the cell membrane. This technique determines a one-dimensional electron density profile along the surface normal, which describes the lipid monolayer as well as the changes in the electron density upon protein binding. Results obtained by other membrane proteins have been interpreted in terms of structural changes of the lipid system caused by the protein bonding [26–30]. A complementary method to investigate lipid–protein interaction at interfaces is neutron reflectivity. This technique has developed rapidly in the last years for studying biological systems [31–33]. Through hydrogen/deuterium isotopic substitution in the lipid system, the refraction index distribution at interfaces can be

* Corresponding author. Division of Soft Matter Physics, Faculty for Physics and Earth Sciences, University of Leipzig, Linnéstr. 5, D-04103 Leipzig, Germany. Fax: +49 341 9732479.
E-mail address: dietrich@physik.uni-leipzig.de (U. Dietrich).

0005-2736/$ – see front matter © 2009 Elsevier B.V. All rights reserved.
doi:10.1016/j.bbamem.2009.04.001

modified, which serves as a tool to detect how the protein affects the structure of the phospholipid monolayer.

In the study presented here, film balance, fluorescence microscopy, x-ray and neutron reflectivity studies were applied to a membrane model system containing DPPC and PIP_2 spread on a reservoir of MARCKS (151–171) peptide. The structural information, extracted from the reflectivity data in combination with the results from fluorescence microscopy indicate clearly that the structure of the lipid monolayer depends on the interaction with the MARCKS peptide: The PIP_2 molecules are existent in an arbitrary uniform distribution in the mixed peptide free monolayer, whereas the PI (4,5) group extends up to 15 Å into the subphase in free state. The interaction with the MARCKS peptide, however, yields a tilt of the PI (4,5) groups of PIP_2 toward the membrane interface.

2. Materials and methods

2.1. Chemicals

1,2-Dipalmitoyl-sn-glycero-3-phosphocholine (DPPC) and 1,2-Dipalmitoylphosphatidyl-inositol 4,5-diphosphate (PIP_2) from Sigma (Germany), and 1,2-Dipalmitoyl-D62-sn-Glycero-3-Phosphocholine-1,1,2,2-D4-N,N,N-trimethyl-D9 (DPPC-d75) from Avanti Polar Lipids (Alabaster, USA) respectively, were used as received. DPPC or accordingly DPPC-d75 were dissolved in chloroform/methanol (4:1, Merck, HPLC grade) in a concentration of ~0.6 mM and PIP_2 was dissolved in chloroform/methanol/water (1:1:0.1) in a concentration of ~0.2 mM. The lipid solutions were mixed to the desired PIP_2 content prior spreading. The amount of PIP_2 in the lipid system was always 10 mol%.

The solution of lipid mixture was spread on a subphase, consisting of 100 mM NaCl, 10 mM HEPES and 0.1 mM EDTA (likewise from Sigma), adjusted to pH 7.4 (preparation of the subphase with ultra-pure water, obtained from a Milli-Q system (Millipore, Schwalbach, Germany) with a residual specific resistance of 18.2 MΩ cm). The MARCKS (151–175) peptide, obtained as lyophilized powder from AnaSpec (San Jose, USA), was also used as received. For the preparation, the peptide was dissolved in ultra-pure water and was given directly into the subphase with a concentration of 25 nM of the full molecule at the corresponding experiments.[1] So a uniform distribution of the peptide in the subphase and also in the monolayer can be assumed.

2.2. Experiments

2.2.1. Isotherms and fluorescence microscopy

A well-established method for studying the lateral organization of lipids in monolayers is fluorescence microscopy combined with information about the phase behavior of the lipids depending on the lateral pressure. That permits a characterization of the monolayers on a micrometer scale depending on their composition and interaction with membrane binding components like peptides or proteins [34].

Surface pressure-area isotherms of the monolayers were collected using a thermostated Langmuir film balance of homemade design featuring an ash-free filter paper as Wilhelmy plate at a subphase temperature of 20 °C. The studies of the mesoscopic morphology of the monolayer were performed with a Zeiss Axiotech Vario epifluorescence microscope (dye: NBD C_{12}-HPC, Molecular Probes), attached to the film balance [35]. The dissolved DPPC or DPPC/PIP_2 mixtures were spread on the subphase and the solvent was allowed to evaporate for at least 10 min. The monolayers were compressed typically at a barrier speed that correspond to approximately 2 $Å^2$ /(molecule min); the surface pressure π was continuously monitored.

2.2.2. Scattering experiments

While the preceding experiments give an insight into the monolayer organization in the x–y plane on a micrometer scale—by means of scattering experiments we can get detailed structural information on quasi-molecular scale perpendicular to the surface.

X-ray reflectivity measurements were carried out at the undulator beamline BW1 of the DORIS III bypass at HASYLAB (DESY, Hamburg, Germany). The experimental setup has been described in [27]. The x-ray wavelength was between $\lambda = 1.38$ and 1.45 Å and the maximum footprint on the sample was ~2 mm × 50 mm. The custom built Langmuir film balance was incorporated in a thermostated ($T = 20$ °C), gas-tight aluminum container with Kapton windows, which are transparent for x-ray radiation. A polished Pyrex glass block in the subphase flattened the surface waves of the sample in the film balance. All measurements were performed with a Helium atmosphere over the sample film.

The same setup was used to obtain grazing incidence x-ray diffraction (GIXD) data. This diffraction measurement allows a more direct access to structural information on the lipid chains and gives therefore a possibility to validate the reflectivity data. The experimental arrangement was switched automatically between GIXD and reflectivity without altering the monolayer within some minutes. The scattered signal was collected with a Soller collimated linear detector stepped along the scattering angle 2Θ. The detailed setup can be found in [30]. During data recording, the monolayer was shifted to prevent beam damage in both experiments.

The neutron reflectivity measurements were carried out at the AMOR time-of-flight neutron reflectometer beamline at the Swiss Spallation Neutron Source SINQ (Paul Scherrer Institut, Villigen, Switzerland). The experimental setup has been described in [36,37]. The measurements were performed using a film balance identical in construction just like at BW1 at HASYLAB except the Kapton windows were replaced against aluminum windows, which are transparent for cold neutrons.

2.2.3. Data analysis

The x-ray data evaluation was performed with the Volume-Restricted Distribution Function (VRDF) approach as an explicit chemical model. The fundamental ideas of the VRDF approach are described in [38,39]. The results allow more detailed structural information on the monolayer along the surface normal z.

The model divides the molecule in movable fragments, where their positioning is restricted by the available volume in a certain slice, calculated from the molecular area obtained from the isotherm measurement and the slice thickness. The chosen molecular fragments are the acyl chains, the carbonyl groups together with the glycerol backbone, the phosphate group and the choline group according to Armen et al. [40], or the second phosphate group contributed through the PI(4,5) group of the PIP_2, respectively. The sugar fragment is neglected due to the very similar electron density compared to the one of water.

The lipid chains are treated as one homogeneous layer of width d_{ch}, smeared by the global roughness σ_{CW}, which accounts for the capillary waves [38,39]. Thus, the electron density (ED) of the lipid chains ρ^{ch}_{el} is given by:

$$\rho^{ch}_{el} = \frac{Z_{ch}}{2A_{lipid}d_{ch}}\left(\mathrm{erf}\left(\frac{z + d_{ch}}{\sqrt{2}\sigma_{cw}}\right) - \mathrm{erf}\left(\frac{z}{\sqrt{2}\sigma_{cw}}\right)\right) \quad (1)$$

whereas Z_{ch} is the number of electrons of the lipid chains and A_{lipid} is the mean area per lipid molecule. The layer of lipid headgroups is divided into three submolecular fragments, the carbonyls and the

[1] By means of isotherm measurements we could verify a saturation of the monolayer with this concentration of MARCKS (151–175) peptide.

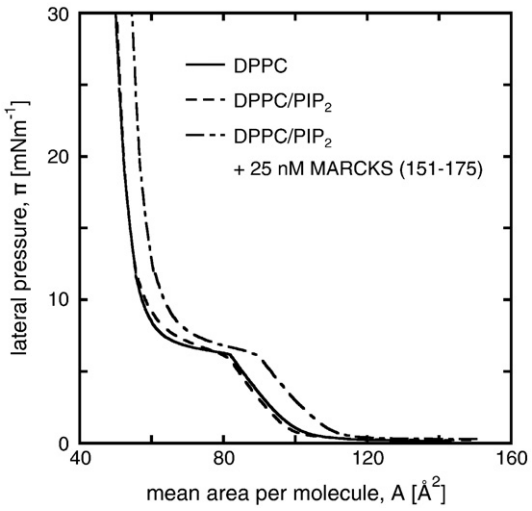

Fig. 1. Surface pressure-area isotherms. Pure DPPC and DPPC/PIP_2 mixture on buffer and DPPC/PIP_2 mixture on buffer containing 25 nM MARCKS (151–175), T = 20 °C.

glycerol group, the phosphate group and the terminal end of the phospholipid headgroup as a third one. The ED $\rho_{el}^{j}(z)$ and the volume distribution $v_j(z)$ of a fragment j along the surface normal z is given by [38,39]:

$$\rho_{el}^{j}(z) = \frac{Z_j}{A_{lipid}} \frac{1}{\sigma\sqrt{2\pi}} \exp\left(-\frac{\left(z-z_j\right)^2}{2\sigma^2}\right) \quad (2)$$

$$v_j(z) = \frac{V_j}{A_{lipid}} \frac{1}{\sigma\sqrt{2\pi}} \exp\left(-\frac{\left(z-z_j\right)^2}{2\sigma^2}\right) \quad (3)$$

with

$$\sigma = \sqrt{\sigma_{cw}^2 + \sigma_{int}^2} \quad (4)$$

whereas Z_j is the number of electrons in the fragment and V_j is the volume. The number of electrons in the fragments is known and the fragment volumes are taken from [40]. The fragment position z_j along the surface normal z is represented by a Gaussian distribution with the width σ. This describes the deviation from their average position due to capillary waves σ_{cw} at the surface and thermal disorder σ_{int} within the monolayer. The fitting parameters of the model are the global and the intrinsic roughness, σ_{cw} and σ_{int}, the width of the chain layer, d_{ch}, and the positions of the second and third fragments. For reducing the number of fit parameters, the glycerol/carbonyl fragment is attached to the lower end of the lipid chains at the position $z_{GC} = \sigma_{int}$ [41]. However, due to the insertion of an additional lipid into the monolayer, it is necessary to split the third fragment to take the molecular composition into consideration. One part becomes the choline group of DPPC and the other the PI(4,5) group of PIP_2. For the fitting procedure, both parameters of this fragment are weighted according to their fraction in the lipid mixture. The void volume in the headgroup region is filled with subphase to meet a complete volume condition. Though, because the sugar moiety of the PIP_2 was neglected, the number of electrons "filled" in this volume is partly from the inositol group.

The calculations of the neutron reflectivity curves were carried out using Parratt's dynamical approach [42] implemented as a simple two box model. Due to the limited accessible momentum transfer available in the neutron scattering experiment the following two parameters were fixed: the chain length data were taken from the x-ray results and their neutron scattering length density was used as found elsewhere [43].

3. Results

3.1. Isotherms

The surface pressure-area isotherms for the pure DPPC monolayer, the mixed DPPC/PIP_2 monolayer on the subphase without MARCKS (151–175) and the mixed monolayer with MARCKS (151–175) in the subphase are shown in Fig. 1. There is no significant influence of PIP_2 on the phase behavior and the mean area per lipid molecule compared to the pure DPPC monolayer. In contrast, the interaction of MARCKS (151–175) with the monolayer leads to a significant increase of the mean area per molecule. This increase is obviously caused by the partial insertion of the peptide into the monolayer [7,9,18,19,21,23,44]. The shape of this isotherm is rather identical to the DPPC isotherm, indicating that integration of the MARCKS (151–175) peptide into the monolayer shows no observable influence on the lipid phase. The DPPC phase is obviously undisturbed and the additional molecular area per lipid results from a separate phase caused by the interaction of the peptide with the monolayer.

3.2. Fluorescence microscopy

The influence of the MARCKS effector domain on the monolayer can be characterized with fluorescence microscopy, a sensitive tool for monitoring the lateral organization of monolayers. The phase separation of the monolayer in a condensed lipid phase and a dye rich fluid phase permits an insight in the lateral organization of the

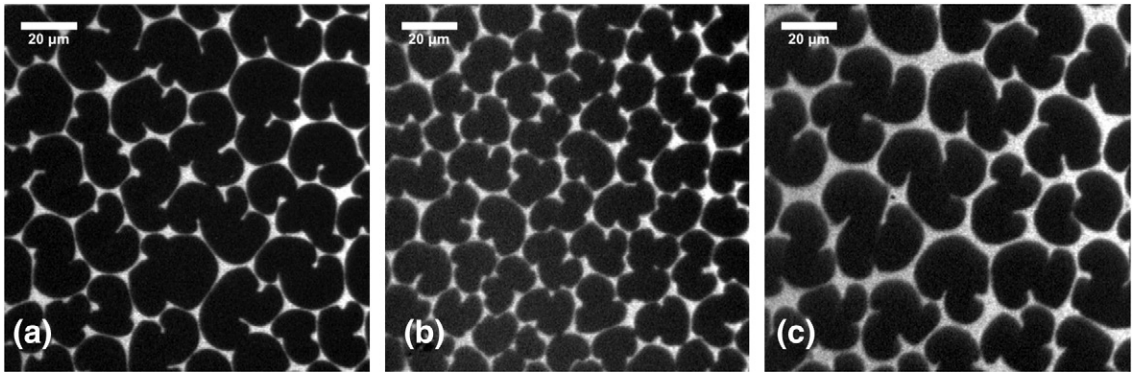

Fig. 2. Fluorescence micrographs of the monolayers. (a) DPPC and (b) DPPC/PIP_2 mixture on buffer and (c) DPPC/PIP_2 mixture with 25 nM MARCKS (151–175) in the subphase at $\pi = 15$ mNm^{-1}, $T = 20$ °C.

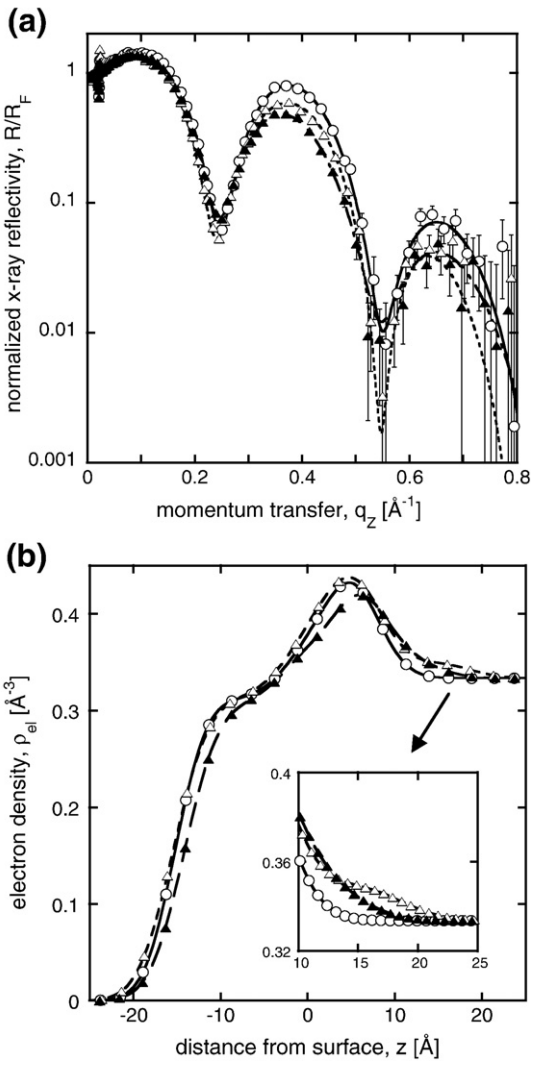

Fig. 3. X-ray reflectivity. (a) Fresnel normalized x-ray reflectivity curves at lateral pressure $\pi = 30$ mNm^{-1}, $T = 20$ °C, and (b) the corresponding VRDF-derived electron density profiles. (○) DPPC, (△) DPPC/PIP_2 and (▲) DPPC/PIP_2 with 25 nM MARCKS (151–175) in the subphase (the end of the hydrophobic chains defines the origin of the z-axis).

three investigated systems. Fig. 2 shows the three systems at a surface pressure of 15 mNm^{-1} at 20 °C.[2] This pressure is above the main phase transition of DPPC from the liquid-expanded to the liquid-condensed phase. The main part of the monolayers is in a condensed highly packed state (dark) in coexistence with remains of disordered loosely packed regions (bright). Due to the integration of acidic lipids into DPPC monolayer a phase separation in a condensed DPPC phase and a disordered PIP_2 rich phase occurs presumably. The high charge of the PIP_2 leads to a repulsive interaction within the monolayer [45], so that these molecules are existent in a random distribution. That disorganization yields a decrease of the domain size in relation to the pure DPPC monolayer, while the domains retrieve a comparable size to the pure DPPC monolayer through the interaction of MARCKS (151–175) with the PIP_2 containing monolayer. However, a larger distance between the domains due to the presence of peptide bound at the monolayer can be observed. According to recent publications, the addition of the highly positively charged MARCKS effector domain yields a strong attraction of the double negatively charged PIP_2 in the plane of the membrane which leads to a lateral accumulation of the polyvalent PIP_2 and therefore to clusters of MARCKS (151–175)/PIP_2 complexes [8,11,46]. The larger distances between the lipid domains could be a hint to a formation of such complexes in the disordered phase. The integration of the MARCKS effector domain into the monolayer is very stable, the lateral surface pressure keeps constant over a long period of time and the domain shape and size as well.

The change of the mean molecular area parallel to the change of the lateral distribution of the domains demonstrates clearly the interaction between lipid monolayer and peptide. The observation of this interaction occurs on a mesoscopic scale and allows merely qualitative evidence.

3.3. X-ray reflectivity

Advanced structural information about the monolayers, extracted from reflectivity and scattering data, can give some quantitative information about the membrane binding mechanism of MARCKS (151–175). Therefore, x-ray reflectivity measurements were carried out at four different surface pressures above the main phase transition in the fluid condensed phase at 15, 20, 25, and 30 mNm^{-1}. In addition GIXD measurements were carried out at 15 and 30 mNm^{-1}.

Fig. 3a, b shows the Fresnel normalized x-ray reflectivity curves at $\pi = 30$ mNm^{-1} as an example for all three systems and the associated electron density profiles, retrieved from the VRDF approach. Due to the additional phosphate groups in the mixed monolayers a second phosphate layer provides a new contribution to the electron density, caused by the integration of PIP_2 into the monolayer (see inset of Fig. 3b). The interaction of the MARCKS effector domain with the acidic lipids compensates this effect and leads to a broadening and shifting of the phosphate slab. The corresponding calculated structural parameters derived from VRDF modeling of the x-ray data are given in Table 1. The position of the primary phosphate group z_{ph1} is comparable in all three systems. Merely the pure DPPC at $\pi = 15$ mNm^{-1} shows a significant difference with a higher distance to the air–water interface, which could be interpreted as a better ordered structure at this lateral pressure—what, in turn, would imply a lesser order in the monolayer caused by insertion of PIP_2. In contrast to the primary phosphate group, the position of the secondary phosphate group z_{ph2} shows an explicit dependency on the presence of MARCKS (151–175). In the absence of the peptide the PI(4,5) group obviously elongates in direction of the surface normal into the subphase, in agreement with existing literature [47,48]. The interaction of the MARCKS effector domain with the acidic lipids yields a tilt of the PI(4,5) towards the membrane interface—in evidence with the decrease of the distance of the second phosphate group to the interface compared

Table 1
Structural parameter describing the fragment distribution perpendicular to the air–water interface as derived from VRDF modeling of the x-ray data.

System	π/mNm^{-1}	σ_{CW}/Å	σ_{int}/Å	d_{ch}/Å	z_{ph1}/Å	z_N/Å	z_{ph2}/Å
DPPC	15	2.80	1.81	13.87	5.91	−2.23	
	20	2.79	1.84	14.81	4.99	−0.37	
	25	2.82	1.43	15.18	5.00	0.02	
	30	2.96	1.39	15.44	5.08	0.00	
DPPC/PIP_2	15	2.84	0.91	13.47	4.48	0.73	9.48
	20	3.09	0.93	14.91	4.91	0.19	13.82
	25	3.21	1.22	15.39	5.41	0.06	15.23
	30	3.33	1.15	15.75	5.14	0.05	14.93
DPPC/PIP_2 + 25 nM	15	2.91	0.92	13.10	4.77	0.03	10.80
MARCKS	20	3.01	1.02	13.95	5.31	0.32	11.34
	25	3.13	0.96	14.55	5.68	0.07	12.10
	30	3.10	1.05	15.15	5.08	0.08	12.17

The abbreviations mean σ_{CW}, global roughness; σ_{int}, intrinsic roughness = position of glycerol/carbonyl fragment; d_{ch}, thickness of the lipid chains; z_{ph1}, distance of the phosphodiester group to interface; z_N, distance choline to phosphodiester group; z_{ph2}, distance PI(4,5) group to interface.

[2] At this lateral pressure the domains are still good distinguishable and the monolayer is above the phase transition. An observation at higher lateral pressures does not make sense, because of the dye dissolves into the solution with the lipids.

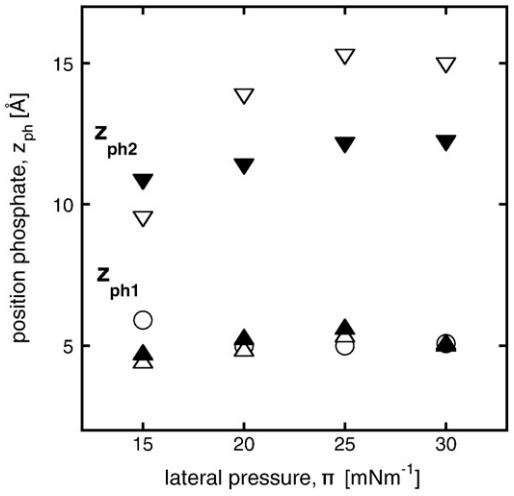

Fig. 4. Phosphate position Z_{ph1} and Z_{ph2} as a function of the lateral pressure π. The position of the primary phosphate group Z_{ph1} is comparable in all three systems. (○) DPPC, (△) DPPC/PIP_2 and (▲) DPPC/PIP_2 with 25 nM MARCKS (151–175) in the subphase. The position of the secondary phosphate group Z_{ph2} shows a dependency on the presence of MARCKS (151–175), here is (▽) DPPC/PIP_2 and (▼) DPPC/PIP_2 with MARCKS (151–175) in the subphase. Without peptide the PI(4,5) group elongates in direction of the surface normal up to 15 Å into the subphase. The interaction of the acidic lipids with the MARCKS effector domain causes a tilt of the PI(4,5) towards the membrane interface, clearly indicated by the decrease of the distance of the second phosphate group to the interface.

to the monolayer without the MARCKS peptide. This could explain the disappearance of the additional phosphate "peak" in the electron density profile. The primary and the secondary phosphate groups are getting closer, which leads to an overlay of the phosphate groups and results in a uniform broader electron density distribution. A graphical summary of the dependency of the position of the phosphate groups z_{ph1} and z_{ph2} on the lateral pressure is given in Fig. 4.

To verify the results obtained from fitting the experimental reflectivity data to the VRDF model, a more direct access to structural information on the lipid chains was offered by grazing incidence x-ray diffraction (GIXD) (e.g. Fig. 5). The lattice data from these experiments are compared in Table 2 with the molecular lipid areas measured by isotherms and the derived data from reflectivity evaluation. Major differences were found in the calculated lipid chain areas and the areas obtained from isotherm measurements. This, however, can be explained because the isotherm measures the

Table 2
Comparison between reflectivity evaluation and GIXD.

System	π/ mNm^{-1}	A_{lipid}/Å^2 isotherm	A_{lipid}/Å^2 GIXD	Tilt angle ϕ/° x-ray	Tilt angle ϕ/° GIXD	FHWM [2,0]/Å^{-1}
DPPC	15	55.6	50.8	43.6	46.1	0.007240
	30	50.1	48.8	36.3	42.2	0.007481
DPPC/PIP_2	15	55.7	50.6	45.3	45.6	0.008269
	30	50.4	49.2	34.7	44.3	0.013263
DPPC/PIP_2 +25 nM MARCKS	15	61.0	50.6	46.8	47.4	0.007434
	30	54.6	48.2	37.7	42.1	0.011728

The tilt angle obtained from the reflectivity data, $\phi = \arccos(d_{ch}/l_{palmitoyl})$, was calculated with $l_{palmitoyl} = 19.15$ Å [43].

entire monolayer while the GIXD focuses only on the crystalline parts of the monolayer. For the reflectivity evaluation the areas from the isotherm were used, which therefore also contain the non-crystalline parts. This explains some differences in the chain tilt angle ϕ obtained in both experiments. At a low lateral pressure of $\pi = 15$ mNm^{-1}, the three systems show a similar behavior. This indicates a homogeneous monolayer structure under these conditions, as visible in both phases in the fluorescence micrograph. A further hint is the width of the diffraction peaks, a measure for the order of the crystalline domains. From the width of the [2,0] peak at the horizon one can deduce a similar state of the order of the chains, whereas the broader peak of the DPPC/PIP_2 indicates a less ordered monolayer. This is also confirmed by the smaller domains in the fluorescence micrograph. The peptide containing system has an explicitly larger difference in the calculated and GIXD-measured lipid area, which indicates a larger fraction of disordered phase, just as well to observe in the fluorescence micrograph. With increasing lateral pressure one should expect a higher ordered monolayer. We observe a contrary behavior at the PIP_2 containing monolayers. Generally, the area fraction of disordered phase is decreasing—the ordered domains are getting closer. The same chain tilt angle for the pure DPPC and the mixed peptide containing monolayer points out a demixing of the ordered and disordered phases. The similar signal, obtained in both systems, must be from the crystalline domains of the DPPC whereas the presence of disordered areas in the peptide containing system leads to a lower intensity and broadening of the signal. While the insertion of PIP_2 into the pure lipid monolayer yields merely a disturbed crystalline phase, the uniform random distribution of PIP_2 leads to imperfections in the monolayer—and thus to a shortening of the correlation length—caused by the

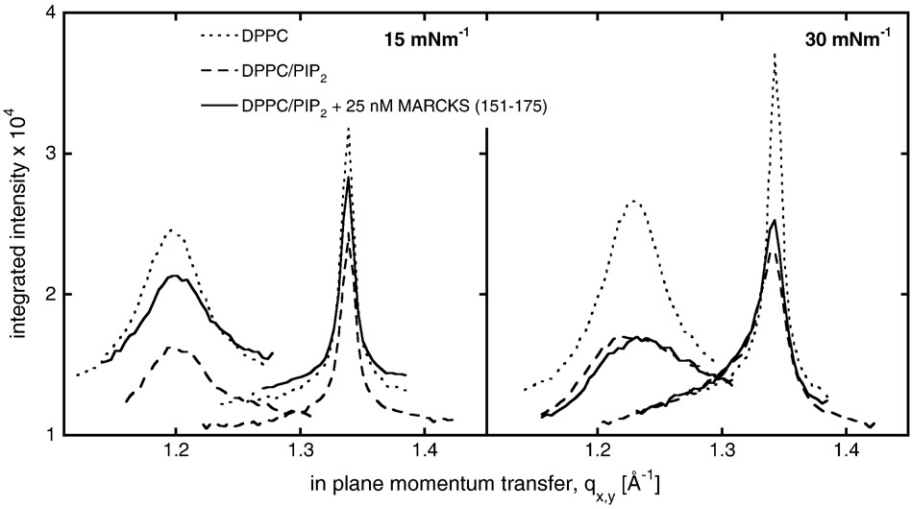

Fig. 5. GIXD measurements of DPPC, DPPC/PIP_2 and DPPC/PIP_2 with 25 nM MARCKS (151–175) at $\pi = 15$ mNm^{-1} and $\pi = 30$ mNm^{-1}. Two Bragg peaks are observed for the three systems, one at the horizon [2,0] and one off horizon [1,1]. The change of the width of the [2,0] peak points to a change of the ordering in the monolayer.

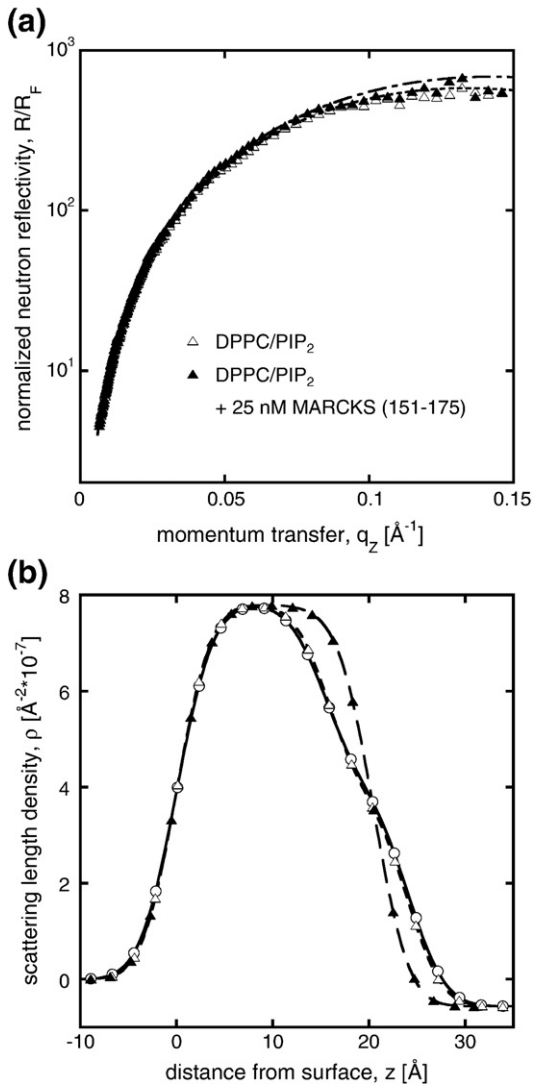

Fig. 6. Neutron reflectivity on buffer (prepared from H_2O). (a) Fresnel normalized neutron reflectivity curves at lateral pressure $\pi = 30$ mNm^{-1} for (△) DPPC/PIP_2 and (▲) DPPC/PIP_2 with 25 nM MARCKS (151–175) in the subphase (because of small differences, the curve for pure DPPC is not shown) and (b) the corresponding scattering length densities ρ; (○) is for DPPC.

elongation of the PI(4,5) group into the subphase, which accounts for a larger tilt angle of the DPPC chains.

3.4. Neutron reflectivity

The neutron reflectivity measurements of the monolayers confirm the preceding x-ray results. While x-ray methods are sensitive to electron density distributions, by contrast variation with H/D isotope exchange neutron scattering can deliver additional information on the molecular arrangements in the monolayer. The Fresnel normalized neutron reflectivity curves (measured at a lateral pressure of 30 mNm^{-1} on H_2O buffer) and the derived neutron scattering length density profiles depicted in Fig. 6 show the influence of the MARCKS (151–175) peptide on the monolayer. The major impact of the MARCKS effector domain on the monolayer is at first a thinning of the surface layer. Furthermore, the distribution of the scattering length density is altered. This is consistent to the x-ray data. Due to the tilt of the PI(4,5) groups in direction of the membrane interface, caused by the interaction with the peptide, the scattering length density is more concentrated at the interface.

4. Discussion

Numerous publications have already dealt with the interaction between acidic membrane lipids and MARCKS protein in terms of their electrostatic interaction. Based on theoretical calculations [10,24,49] and experimental results [10,24,25,50] it was found that the PIP_2 molecules in the membrane are sequestered by the effector domain of the MARCKS protein due to nonspecific electrostatic interactions. Thereby complexes of PIP_2/protein (MARCKS (151–175)) are formed [10]. Beside these studied electrostatic interaction the effector domain of the MARCKS protein penetrates with aromatic amino acid side chains into the hydrocarbon layer and thus shows an extended configuration at the membrane interface. Thereby this protein segment is not altered significantly by the interaction with PIP_2 [19–23].

In the present work we investigate how far the MARCKS (151–175) peptide alters the structure of the membrane interface by adsorption at the mixed lipid monolayer. Hereby we have shown a change of the structural parameters of the lipid matrix depending on the adsorption of the peptide by means of x-ray reflection/diffraction and neutron reflectivity measurements. A schematic depiction of these changes is illustrated in Fig. 7. We were able to show the presence of a uniform distribution of the PIP_2 molecules in the disordered phase of the mixed monolayer, which is consistent with literature [51–53]. This lateral distribution is obviously caused by the perpendicular orientation of the PI(4,5) group to the membrane interface [47,48]. The distance of the phosphate group to the level of the phosphodiester groups of the membrane increases with increasing lateral pressure. At a pressure of 30 mNm^{-1}—comparable to bilayers [54]—the PI(4,5) group is 10 Å below the level of the phosphodiester groups. Consequently, this conformation of the membrane interface is the precondition for the electrostatic interaction of the MARCKS protein with the PIP_2 molecules.

The presence of MARCKS (151–175) in the subphase, i.e. the clusters of its basic residues, produces locally positive electrostatic potentials. Thereby the PIP_2 molecules diffuse laterally within the membrane interface and form electrostatically stabilized complexes with the peptide [49]. The enrichment of the PIP_2 molecules in the disordered phase facilitates their diffusion and therefore the formation of the lipid/peptide complexes occurs in favor

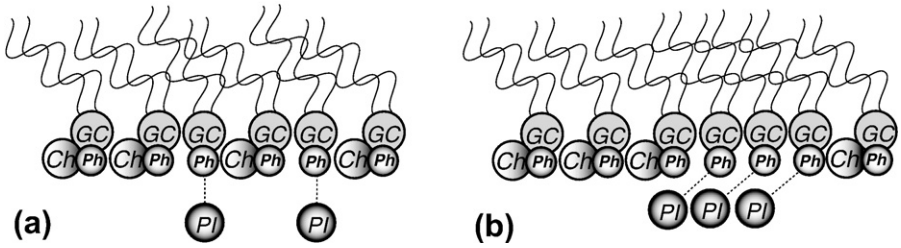

Fig. 7. Sketch of the structure of the mixed monolayer. (a) DPPC/PIP_2 and (b) DPPC/PIP_2 with MARCKS (151–175) interaction, thereby are GC—glycerol/carbonyl fragment, Ch—choline group, Ph—phosphodiester group and PI—PI(4,5) group of PIP_2. The free PI(4,5) elongates perpendicular into the subphase (a) and forms consequently the basis for the lipid/peptide interaction. The presence of MARCKS (151–175) leads to a tilt of the PI(4,5) group towards the membrane interface (b).

presumably in the disordered phase. An indirect evidence of these complexes is the high fraction of disordered phase in the peptide containing system. Comparable experiments with a pure DPPC monolayer did not show an increasing of the disordered phase at presence of MARCKS (151–175) (data not shown). This effect is only attributed to the lipid/peptide interaction.

It is known that the MARCKS (151–175) peptide is located at the polar headgroup region in an extended conformation [23]. Its aromatic amino acid side chains penetrate into the level of the lipid acyl chains, which contribute thus to a stabilization of the lipid matrix [55], and its basic residues elongate into the aqueous phase [23]. The partial penetration of the peptide into the hydrocarbon region of the monolayer causes no obvious changes in the average structure of the lipid matrix. This is consistent with other experiments relating to bilayers [56]. However, the elongation of the PI(4,5) groups out of the lipid matrix into the subphase consequently forms the basis for the lipid/peptide interaction and hence determines the structure and position of the MARCKS effector domain at the membrane interface.

Acknowledgments

We gratefully acknowledge Hans Binder from the Interdisciplinary Centre for Bioinformatics, Leipzig, for helpful discussion and advice. This work was supported by FOR 877 (From Local Constraints to Macroscopic Transport).

References

[1] A. Aderem, Signal transduction and the actin cytoskeleton: the role of MARCKS and profilin, TIBS 17 (1992) 438–443.
[2] P.J. Blackshear, The MARCKS Family of Cellular Protein Kinase C Substrates, J. Biol. Chem. 268 (1993) 1501–1504.
[3] M. Glaser, S. Wanaski, C.A. Buser, V. Boguslavsky, W. Rashidzada, A. Morris, M. Rebecchi, S.F. Scarlata, L.W. Runnels, G.D. Prestwich, J. Chen, A. Aderem, J. Ahn, S. McLaughlin, Myristoylated Alanine-rich C Kinase Substrate (MARCKS) Produces Reversible Inhibition of Phospholipase C by Sequestering Phosphatidylinositol 4,5-Biphosphate in Lateral Domains, J. Biol. Chem. 271 (1996) 26184–26193.
[4] F. Wohnsland, A.A.P. Schmitz, M.O. Steinmetz, U. Aebi, G. Vergères, Interaction between Actin and the Effector Peptide of MARCKS-related Protein, J. Biol. Chem. 275 (2000) 20873–20879.
[5] J.H. Hartwig, M. Thelen, A. Rosen, P.A. Janmey, A.C. Nairn, A. Aderem, MARCKS is an actin filament crosslinking protein regulated by protein kinase C and calcium-calmodulin, Nature 356 (1992) 618–622.
[6] T. Laux, K. Fukami, M. Thelen, T. Golub, D. Frey, P. Caroni, GAP43, MARCKS, and CAP23 Modulate PI(4,5)P_2 at Plasmalemmal Rafts, and Regulate Cell Cortex Actin Dynamics through a Common Mechanism, J. Cell Biol. 149 (2000) 1455–1471.
[7] A. Arbuzova, L. Wang, J. Wang, G. Hangyás-Milháyné, D. Murray, B. Honig, S. McLaughlin, Membrane Binding of Peptides Containing Both Basic and Aromatic Residues. Experimental Studies with Peptides Corresponding to the Scaffolding Region of Caveolin and the Effector Region of MARCKS, Biochemistry 39 (2000) 10330–10339.
[8] J. Wang, A. Arbuzova, G. Hangás-Milháyné, S. McLaughlin, The Effector Domain of Myristoylated Alanine-rich C Kinase Substrate Binds Strongly to Phosphatidylinositol 4,5-Biphosphate, J. Biol. Chem. 276 (2001) 5012–5019.
[9] A. Arbuzova, J. Wang, D. Murray, J. Jacob, D.S. Cafiso, S. McLaughlin, Kinetics of Interaction of the Myristoylated Alanine-rich C Kinase Substrate, Membranes, and Calmodulin, J. Biol. Chem. 272 (1997) 27167–27177.
[10] J. Wang, A. Gambhir, G. Hangyás-Mihályné, D. Murray, U. Golebiewska, S. McLaughlin, Lateral Sequestration of Phosphatidylinositol 4,5-Biphosphate by the Basic Effector Domain of Myristoylated Alanine-rich C Kinase Substrate Is Due to Nonspecific Electrostatic Interactions, J. Biol. Chem. 277 (2002) 34001–34412.
[11] S. McLaughlin, J. Wang, A. Gambhir, D. Murray, PIP_2 and Proteins: Interactions, Organization, and Information Flow, Annu. Rev. Biophys. Biomol. Struct. 31 (2002) 151–175.
[12] S. Ohomori, N. Sakai, Y. Shirai, H. Yamamoto, E. Miyamoto, N. Shimizu, N. Saito, Importance of Protein Kinase C Targeting for the Phosphorylation of Its Substrate, Myristoylated Alanine-rich C-kinase Substrate, J. Biol. Chem. 275 (2000) 26449–26457.
[13] J. Kim, P.J. Blackshear, J.D. Johnson, S. McLaughlin, Phosphorylation Reverses the Membrane Association of Peptides that Correspond to the Basic Domains of MARCKS and Neuromodulin, Biophys. J. 67 (1994) 227–237.
[14] S. McLaughlin, A. Aderem, The myristoyl-electrostatic switch: a modulator of reversible protein-membrane interactions, TIBS 20 (1995) 272–276.
[15] J.T. Seykora, M.M. Myat, L.-A.H. Allen, J.V. Ravetch, A. Aderem, Molecular Determinants of the Myristoyl-electrostatic Switch of MARCKS, J. Biol. Chem. 271 (1996) 18797–18802.
[16] M.M. Myat, S. Anderson, L.-A.H. Allen, A. Aderem, MARCKS regulates membrane ruffling and cell spreading, Curr. Biol. 7 (1997) 611–614.
[17] A. Arbuzova, D. Murray, S. McLaughlin, MARCKS, membranes, and calmodulin: kinetics of their interaction, Biochim. Biophys. Acta 1376 (1998) 369–379.
[18] D. Murray, A. Arbuzova, B. Honig, S. McLaughlin, The Role of Electrostatic and Nonpolar Interactions in the Association of Peripheral Proteins with Membranes, Curr. Top. Membranes 52 (2002) 277–307.
[19] W. Zhang, E. Crocker, S. McLaughlin, S.O. Smith, Binding of Peptides with Basic and Aromatic Residues to Bilayer Membranes, J. Biol. Chem. 278 (2003) 21459–21466.
[20] Z. Qin, D.S. Cafiso, Membrane Structure of Protein Kinase C and Calmodulin Binding Domain of Myristoylated Alanine Rich C Kinase Substrate Determined by Site-Directed Spin Labeling, Biochemistry 35 (1996) 2917–2925.
[21] K. Victor, J. Jacob, D.S. Cafiso, Interactions Controlling the Membrane Binding of Basic Protein Domains: Phenylalanine and the Attachment of the Myristoylated Alanine-rich C-Kinase Substrate Protein to Interfaces, Biochemistry 38 (1999) 12527–12536.
[22] M.E. Rauch, C.G. Ferguson, G.D. Prestwich, D.S. Cafiso, Myristoylated Alanine Rich C Kinase Substrate (MARCKS) Sequesters spin-labeled Phosphatidylinositol 4,5-Biphosphate in Lipid Bilayers, J. Biol. Chem. 266 (2002) 14068–14076.
[23] J.F. Ellena, M.C. Burnitz, D.S. Cafiso, Location of the Myristoylated Alanine Rich C Kinase Substrate (MARCKS) Effector Domain in Negatively Charged Phospholipid Bicells, Biophys. J. 85 (2003) 2442:2448.
[24] A. Gambhir, G. Hangyás-Mihályné, I. Zaitseva, D.S. Cafiso, J. Wang, D. Murray, S.N. Pentyala, S.O. Smith, S. McLaughlin, Electrostatic Sequestration of PIP_2 on Phospholipid Membranes by Basic/Aromatic Regions of Proteins, Biophys. J. 86 (2004) 2188–2207.
[25] L. Rusu, A. Gambhir, S. McLaughlin, J. Rädler, Fluorescence Correlation Spectroscopy Studies of Peptide and Protein Binding to Phospholipid Vesicles, Biophys. J. 87 (2004) 1044–1053.
[26] H. Möhwald, H. Baltes, M. Schwendler, C. Helm, G. Brezesinski, H. Haas, Phospholipid and Protein Monolayers, Jpn. J. Appl. Phys. 34 (1995) 3906–3913.
[27] T.R. Jensen, K. Kjaer, Structural Properties and Interactions of Thin Films at the Air-Liquid Interface Explored by Synchrotron X-ray Scattering, Studies in Interface Sci. 11 (2001) 205–254.
[28] A.G. Lee, Lipid-protein interactions in biological membranes: a structural perspective, Biochim. Biophys. Acta 1612 (2003) 1–40.
[29] M. Weygand, B. Wetzer, D. Pum, U.B. Sleytr, N. Cuvillier, K. Kjaer, P.B. Howes, M. Lösche, Bacterial S-Layer Protein Coupling to Lipids: X-Ray Reflectivity and Gracing Incidence Diffraction Studies, Biophys. J. 76 (1999) 458–468.
[30] K.Y.C. Lee, J. Majewski, T.L. Kuhl, P.B. Howes, K. Kjaer, M.M. Lipp, A.J. Waring, J.A. Zasadzinski, G.S. Smith, Synchrotron X-Ray Study of Lung Surfactant-Specific Protein SP-B in Lipid monolayers, Biophys. J. 81 (2001) 572–585.
[31] C. Naumann, C. Dietrich, A. Behrisch, T. Bayerl, M. Schleicher, D. Bucknall, E. Sackmann, Hisactophilin-Mediated Binding of Actin to Lipid Lamellae: A Neutron Reflectivity Study of Protein Membrane Coupling, Biophys. J. 71 (1996) 811–823.
[32] J. Majewski, T.L. Kuhl, M.C. Gerstenberg, J.N. Israelachvili, G.S. Smith, Structure of Phospholipid Monolayers Containing Poly(ethylene glycol) Lipids at the Air-Water Interface, J. Phys. Chem. B 101 (1997) 3122–3129.
[33] J. Penfold, Neutron scattering for surface characterization, Curr. Sci. 78 (2000) 1458–1466.
[34] M. Dyck, M. Lösche, Interaction of the Neurotransmitter, Neuropeptide Y, with Phospholipid Membranes: Film Balance and Fluorescence Microscopy Studies, J. Phys. Chem. B 110 (2006) 22143–22151.
[35] P. Krüger, M. Schalke, Z. Wang, R.H. Notter, R.A. Dluhy, M. Lösche, Effect of hydrophobic surfactant peptides SP-B and SP-C on binary phospholipid monolayers. I. Fluorescence and dark-field microscopy, Biophys. J. 77 (1999) 943–952.
[36] D. Clemens, P. Gross, P. Keller, N. Schlumpf, M. Könnecke, AMOR – the versatile reflectometer at SINQ, Physica B 276-278 (2000) 140-141
[37] M. Gupta, T. Gutberlet, J. Stahn, P. Keller, D. Clemens, AMOR – the time-of-flight neutron reflectometer at SINQ/PSI, Pranama-J. Physics 63 (2004) 57–63.
[38] M. Schalke, P. Krüger, M. Weygand, M. Lösche, Submolecular organization of DMPA in surface monolayers: beyond the two-layer model, Biochim. Biophys. Acta 1464 (2000) 113–126.
[39] M. Schalke, M. Lösche, Structural models of lipid surface monolayers from x-ray and neutron reflectivity measurements, Adv. Colloid Interface Sci. 88 (2000) 243–274.
[40] R.S. Armen, O.D. Uitto, S.E. Feller, Phospholipid Component Volumes: Determination and Application to Bilayer Structure Calculations, Biophys. J. 75 (1998) 734–744.
[41] M. Dyck. Lipid Headgroup Organization and Interaction of Neuropeptide Y with Phospholipid Membranes, PhD 2006, Universität Leipzig.
[42] L.G. Parratt, Surface studies of solids by total reflection of x-rays, Phys. Rev. 95 (1954) 359–369.
[43] D. Vaknin, K. Kjaer, J. Als-Nielsen, M. Lösche, Structural properties of phosphatidylcholine in a monolayer at the air/water interface, Biophys. J. 59 (1991) 1325–1332.
[44] G. Bähr, A. Diederich, G. Vergères, M. Winterhalter, Interaction of the Effector Domain of MARCKS and MARCKS-Related Protein with Lipid Membranes Revealed by Electric Potential Measurements, Biochemistry 37 (1998) 16252–16261.
[45] I. Levental, P.A. Janmey, A. Cebers, Electrostatic Contribution to the Surface Pressure of Charged Monolayers Containing Polyphosphoinositide, Biophys. J. 95 (2008) 1199–1205.

[46] E. Haleva, N. Ben-Tal, H. Diamant, Increased Concentration of Polyvalent Phospholipids in the Adsorption Domain of a Charged Protein, Biophys. J. 86 (2004) 2165–2178.
[47] C. Zhou, V. Garigapati, M.F. Robert, Short-Chain Phosphatidylinositol Conformation and Its Relevance to Phosphatidylinositol-Specific Phospholipase C, Biochemistry 36 (1997) 15925–15931.
[48] J.P. Bradshaw, R.J. Bushby, C.C.D. Giles, M.R. Saunders, Orientation of the Headgroup of Phosphatidylinositol in a Model Biomembrane As Determined by Neutron Diffraction, Biochemistry 38 (1999) 8393–8401.
[49] J. Wang, A. Gambhir, S. McLaughlin, D. Murray, A Computational Model for the Electrostatic Sequestration of $PI(4,5)P_2$ by Membrane-Adsorbed Basic Peptides, Biophys. J. 86 (2004) 1969–1986.
[50] U. Golebiewska, A. Gambhir, G. Hangyás-Mihályné, I. Zaitseva, J. Rädler, S. McLaughlin, Membrane-Bound Basic Peptides Sequester Multivalent (PIP2), but Not Monovalent (PS), Acidic Lipids, Biophys. J. 91 (2006) 588–599.
[51] C. DeWolf, S. Leporatti, C. Kirsch, R. Klinger, G. Brezesinski, Phase separation in phosphatidylinositol/phosphatidylcholine mixed monolayers, Chem. Phys. Lip. 97 (1999) 129–138.
[52] W.J. Foster, P.A. Janmey, The distribution of polyphosphoinositides in lipid films, Biophys. Chem. 91 (2001) 211–218.
[53] F. Fernandes, L.M.S. Loura, A. Fedorov, M. Prieto, Absence of clustering of phosphatidylinositol-(4,5)-biphosphate in fluid phosphatidylcholine, J. Lip. Res. 47 (2006) 1521–1525.
[54] A. Blume, A Comparative Study of the Phase Transitions of Phospholipid Bilayers and Monolayers, Biochim. Biophys. Acta 557 (1979) 32–44.
[55] H. Palsdottir, C. Hunte, Lipids in membrane protein structures, Biochim. Biophys. Acta 1666 (2004) 2–18.
[56] K.V. Damoran, K.M. Merz, B.P. Gaber, Interaction of Small Peptides with Lipid Bilayers, Biophys. J. 69 (1995) 1299–1308.